Optimization of part orientation and adapted supports for manufacturing of ceramic parts by stereolithography using finite element simulations

V. Pateloup[a*], P. Michaud[a], T. Chartier[a]

[a] CNRS, University of Limoges, Institute of Research for Ceramics (IRCER), UMR 7315, European Ceramics Center, Limoges, France

[*] Corresponding author: Vincent Pateloup

[*] Corresponding author E-Mail: vincent.pateloup@unilim.fr

Keywords

Stereolithography, Ceramic, Modelling, Scraping, Optimal orientation

Abstract

The manufacturing of ceramic green parts using the stereolithography process requires several steps, which can each influence the mechanical properties of the printed parts: dimensional precision, surface roughness and mechanical strength. The part orientation with respect to the working plan and adapted supports are key points to avoid the failure of the green part during its construction. Indeed, mechanical forces generated during the spreading of thin layers of ceramic suspension generate significant loads on the green part being printed and may displace it or lead to its rupture. It is then crucial to choose a part orientation that minimize these effects and to create adapted supports that can hold the scraping loads. In this respect, a finite element simulation of scraping is performed to analyze the best green part orientation and adapted supports during the stereolithography process. A specific and original experiment is developed to identify the scrapings loads, essential as input data for the simulation. Modellings confirms that the orientation of the support greatly influences the deformations of the green part and highlights the importance of the support stiffness that absorb the scraping forces.

1. Introduction

The stereolithography process, initially developed for polymeric materials [1] makes it possible to manufacture objects of complex shapes while guaranteeing a reduction in time between design and manufacture. Today, useful ceramic parts can be produced by curing ceramic-filled resins using the vat photopolymerization process. This technique permits to manufacture ceramic parts with high complex architectures, a very good dimensional resolution, a good surface roughness, mechanical properties and sintered densities similar to those obtained by conventional shaping methods that are

not able to produce highly complex structures with detailed features [2-3]. This additive process is used in many fields such as aerospace, automotive industry, biomedical, electronics, energy, … [4-6]. Although the stereolithography process is reliable and the accuracy of printed products is among the highest of AM, the quality (in terms of dimensional accuracy, surface roughness and mechanical behavior) can be increased by improving the understanding and the modelling of the different physical behavior of the process [7-8].

The general principle of the stereolithography process is to photopolymerize a thin layer of ceramic paste/suspension using a UV laser. The UV-reactive ceramic system consists of a dispersion of ceramic particles in a curable resin with the addition of a photo-initiator. The resin used is generally a mixture of monomers/oligomers. The photo-initiator makes it possible to generate free radicals and to initiate the polymerization of the ceramic-based system under the effect of light [9]. When photopolymerization of the cross-sectional pattern of one layer is finished, the support table moves down or up, depending on the configuration of the machine (bottom-up or top-down), the desired layer thickness in order to manufacture the next layer. The process is repeated for all layers. Frequently a scraper, or doctor blade, is used to spread the layers that generates scraping loads, which must be supported by the green printed part and its associated supports.

The steps of orienting the part on a production platform and creating supports, although being common to all additive manufacturing processes, are specific to each process. In the specific case of stereolithography process, i) the spreading of a thin layer (i.e. 25 to 100 μm) generates mechanical shear stresses on the previously built green part which can cause its failure, ii) the number and the positioning of the supports influence the mechanical behavior of the part subjected to an external mechanical load both in terms of deformations of the part itself as well as of reaction of connection with the support table which can degrade the dimensional quality of the piece, lead to warping or manufacturing failure.

Concerning the spreading of the thin layers, the analogy with the ceramic tape casting process can be done. Some studies have been performed concerning the influence of the effect of doctor blade on the spreading and on the rheology of the slurry. Studying the production of SiC membranes by tape casting, Gorso et al. [10] have shown that the most important parameters that influence the thickness of the deposited layer are the gap between the blade and the support and the casting speed, then the shear rate imposed to the slurry. Svec et al. [11] have investigated the influence of processing parameters like casting speed, hydrostatic pressure and blade geometry during the tape casting process on local flow behaviour of a slurry in the tape casting head by means of laser doppler velocimetry. They demonstrated the great influence of the geometry of the doctor blade on the flow velocity profiles of the suspension during tape casting and of the local flow on the characteristics of the green tape. Polfer et al. [12] have focused their work, both numerically and experimentally, on the influence of the shape of the doctor blade on the shear rate imposed to the slurry as well as on the orientation of anisotropic ceramic particles. They reported that the flow is essentially a Couette flow (like illustrated

in Fig.2a). More recently, Timurkutluk et al. [13] investigated the impact of the doctor blade gap on mechanical, microstructural and electrochemical properties of tape cast NiO/YSZ SOFC anode supports. They observed that the doctor blade gap could lead to different microstructural characteristics of the green sheets (porosity and pore size).

If we now consider AM, several studies have investigated the optimal orientation problem of parts during AM process. Indeed, part-building orientation is one of the most important factors in 3D layered manufacturing, which can affect the quality of parts as well as the fabrication time and cost. In many studies, the optimal orientation is sought topologically in order to minimize surface defects related to layer-by-layer deposition, build time and the complexity of support structures [14-19]. The mechanical constraints related to the process, which generate stresses on green parts during manufacturing by stereolithography, have been studied [20-21]. The authors analyzed, in particular, the mechanism of force separation via numerical and analytical cohesive zone models. In all cases, the reported results were carried out, for those concerning the stereolithography process, on unfilled photosensitive resins and not on ceramic loaded suspensions. The rheology of these non-loaded systems, as well as the laws of material behavior of the polymeric parts produced being very different, the results cannot be transposed to the printing of ceramic green parts by stereolithography. Recently, Hada et al. [22] have studied the effects of the printing direction on the respect of the geometry and precision of resin dentures build by stereolithography. Three different printing directions $(0^{\circ}, 45^{\circ}, 90^{\circ})$ were investigated. For SLA 3D printer and photopolymer resin used in their study, the authors showed that the better results and the most favorable surface adaptation occurred when the printing direction is 45°.

The ceramic stereolithography process imposes stresses to the part being constructed during the spreading of each thin layer of ceramic suspension depending on his own rheological behavior and spreading parameters (speed, gap) for a given blade geometry. The thin film undergoes a significant shearing, which generates a resultant of the shear load applied to the layer of the part under manufacturing. This force may, depending on the orientation of the part on the support table, causes permanent deformation of the part, rupture of thin sections or detachment of the part from its support. These cases necessarily lead to the rejection of the part during manufacture.

This work aims to optimize the part orientation in order to minimize deformation the green part to avoid its failure and to minimize the amount of matter for supports. The first part of this paper is devoted to evaluating experimentally, using a specific device integrated into a stereolithography machine, the loads generated during the scraping step to spread a thin layer of a high viscosity ceramic suspension. A Greco-Latin square design of experiments was therefore carried out on a commercial photopolymerizable Al_2O_3 suspension to sweep all manufacturing parameters by varying the layer thickness, the speed of the blade, the frequency of oscillations of the blade and the quantity of suspension used. In a second time and in order to determine the relative displacements of the printed part and its supports in the directions of stress during the spreading of the ceramic suspension, a finite

element modelling has been developed. Various orientations of the part and its supports on the table plate have been studied to determine the optimal orientation and the optimal number of supports, which minimize part displacement and therefore maximize a satisfying building of the part.

2. Experimental

2.1. Method

2.1.1. Materials and process

As with any 3D printing technique, a digital file is necessary and can be generated through a CAD software to describe the geometry of the desired part. This file, often in STL format, is transmitted to the printing software, where a slicer cuts the model in thin layers with a fixed thickness. Once the file is sliced, the different printing paths are computed and the obtained instructions are then sent to the machine. Among the different components of the top-down stereolithography machine used (Fig.1), there is a suspension tank, a mobile support table ($\vec{z}$ axis), a scraping system ($\vec{x}$ axis), a UV laser beam, focusing optics and a galvanometric mirror driven by computer ($\vec{x}$ and $\vec{y}$ axes). The laser beam scans the surface of the ceramic filled curable resin according to the digital 3D model supplied to the printer. After the first layer has polymerized in the desired cross-sectional pattern, the platform moves down from a layer thickness and a new layer of suspension is deposited on the surface. An oscillating scraper ($\vec{x}$ axis for the movement of displacement and $\vec{y}$ axis for the oscillating movement) is used to drag the suspension over the working plane, which ensures a better surface finish of the deposited layer and recoating of the polymerized pattern. A new cross-sectional pattern is then solidified. The part is built layer upon layer.

The alumina ceramic suspension, used in this work, is loaded at 58 $vol\%$ and is commercialized by 3DCeram-Sinto, Limoges, France [23]. The 99.8% pure alumina powder used has a mean particle size of 1.3 µm. The suspension has a shear thinning behavior with a viscosity of 26 Pa.s for a shear rate of 100 s^{-1}. The SLA system with a 355 nm UV laser source (Innolas Nanio AIR 355 3 W) is a machine developed at laboratory.

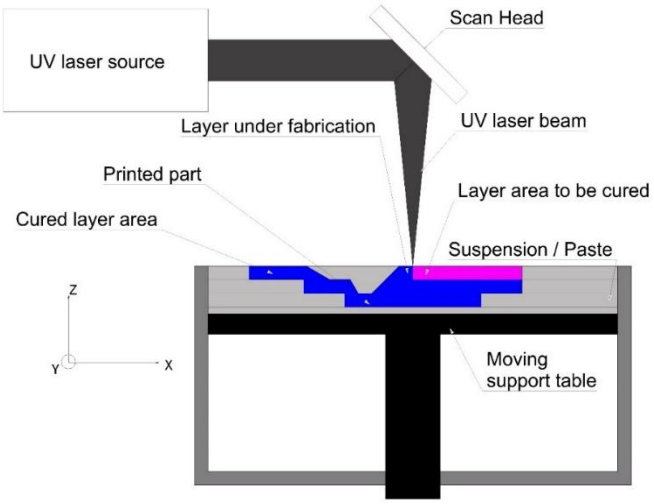
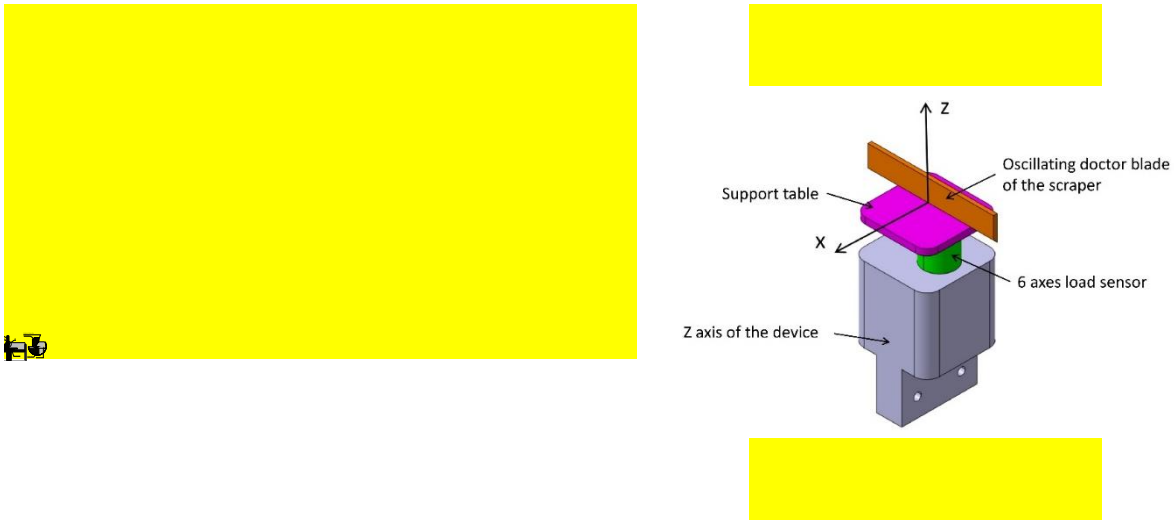


Fig. 1. Top-down stereolithography process used

2.1.2. Identification of scraping loads

The main goal of scraping or recoating step is to deposit a uniform thin layer of ceramic-filled resin (Fig.2a). The underlying challenge is to obtain, as uniform and flat as possible, a curable suspension surface as quickly as possible. However, the ceramic suspension is submitted to shear stresses during the spreading of thin layers, that significantly loads the green printed part due to the high viscosity of the suspension. In order to measure the loads applied to the part during the scraping phase, a specific load sensor (Fig.2b) has been installed on the support table of our stereolithography machine. This load sensor, with a measuring range between 0 and 50 N (force) and between 0 et 1 N.m (torque) with an accuracy of 0.5%, makes it possible to measure the six components of a mechanical load applied between the support table and the rigid frame of the stereolithography machine. In addition, these measured loads will be necessary to test, using numerical modelling, various possible orientations of the part/support assembly on the support table and so to determine the optimal orientation that minimizes deformations and therefore maximizes the chance of building a correct and dimensionally acceptable part.



a) Scraping or recoating of suspension b) Instrumentation of the stereolithography machine

Fig. 2. Scraping process on our stereolithography machine

2.1.3. Design of experiments

A design of experiments, able to sweep all the manufacturing conditions, is carried out to measure the loads applied to one layer of suspension during process with different scraping velocities, oscillating frequency of the doctor blade (amplitude of oscillations near 0,5mm), layer thicknesses and suspension quantities. The evaluation of the influence of these different parameters on the loads applied to the part in construction is conducted as precisely as possible using a Greco-Latin square design of experiments containing four factors with three levels (Table 1). All of the other parameters

constituting the system were fixed for this study (geometry of the blade doctor, size of the support table, ceramic suspension and therefore rheology).

Table 1

Design of experiments

Experiment	E01	E02	E03	E04	E05	E06	E07	E08	E09
Scraping velocity (mm/s) $1 \leq V_{S1} \leq V_{S2} \leq V_{S3} \leq 10$	V_{S1}	V_{S1}	V_{S1}	V_{S2}	V_{S2}	V_{S2}	V_{S3}	V_{S3}	V_{S3}
Frequency (Hz) $0 \leq F_1 \leq F_2 \leq F_3 \leq 200$	F_1	F_2	F_3	F_1	F_2	F_3	F_1	F_2	F_3
Layer thickness (μm) $25 \leq h_1 \leq h_2 \leq h_3 \leq 75$	h_1	h_2	h_1	h_2	h_3	h_1	h_3	h_1	h_2
Suspension quantity (g) $10 \leq S_{q1} \leq S_{q2} \leq S_{q3} \leq 40$	S_{q1}	S_{q2}	S_{q3}	S_{q3}	S_{q1}	S_{q2}	S_{q2}	S_{q3}	S_{q1}

2.2. Experimental results

The evolutions of maximal and average loads in $\vec{x}$ and $\vec{z}$ directions, according to manufacturing parameters and applied to the ceramic suspension via the doctor blade on the support table over its useful surface, are represented in Fig. 3 and Fig. 4, respectively. For each manufacturing parameter, the maximum load in both directions presents the same evolution. The higher the scraping speed and the paste quantity, the more important load. Concerning the layer thickness, the maximum load in both directions increases for a layer thickness between 25 μm and 50 μm, then decreases for a larger layer thickness. The same tendency is observed for oscillating frequencies. For these two last parameters, it can be likely explained by the shear-thinning behavior of the suspension. It can be noticed that the load in $\vec{z}$ direction is twice as high as that in $\vec{x}$ direction. These results demonstrate that the flow of ceramic suspension is not conform to a Couette flow.

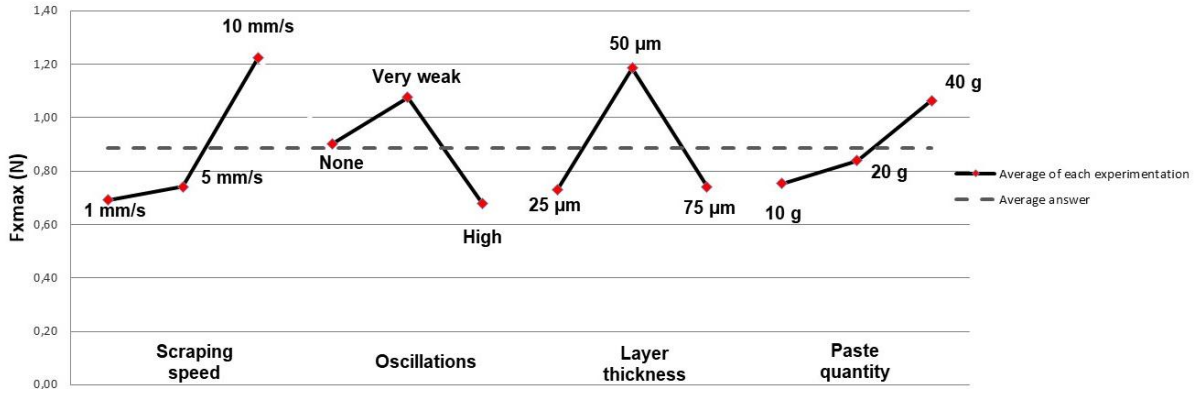


Fig. 3. Maximal loads in the scraping direction ($\vec{x}$)

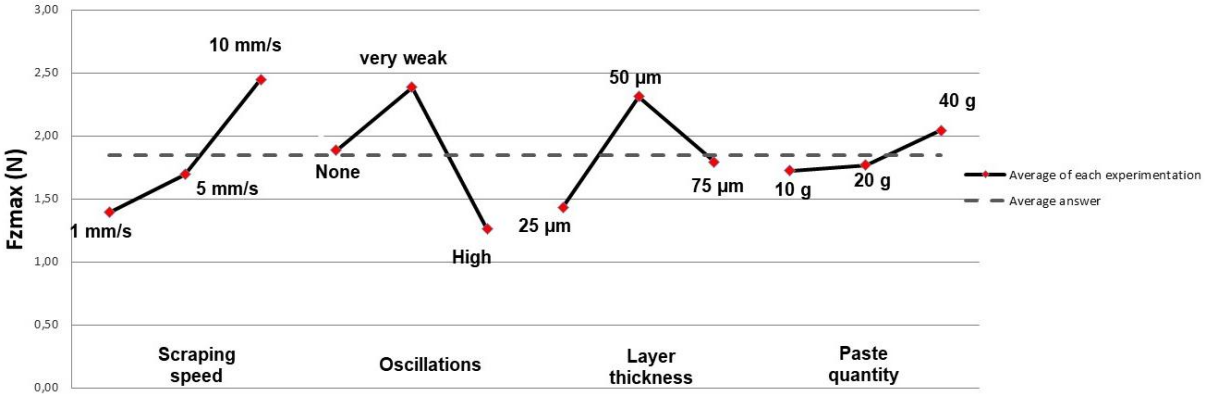


Fig. 4. Maximal loads in the normal direction ($\vec{z}$) to scraping direction

Additional tests were carried out in order to understand and modelling the phenomena involved, in particular the influence of the surface size of the printed part in contact with the blade doctor. A dedicated part (Fig. 5) was used to measure the scraping loads at each layer. The manufacturing parameters used for these tests correspond to those of the E09 experiment (Table 1). During the spreading step, the doctor blade is in contact with a pyramidal part firstly and with two identical pyramidal parts secondly. These pyramids contain 50 layers of 50 µm height. In order to quantify the influence of the surface of the printed part that receive the necessary material for the next layer during it spreading, our proposed test makes it possible to combine:

- the spreading of the ceramic suspension on the surface of a pyramidal part for the first half of the support table then on a double surface of pyramidal parts on the second half of it;
- linear reduction of the previously polymerized surface during the construction thanks to the pyramidal shape of the designed parts.

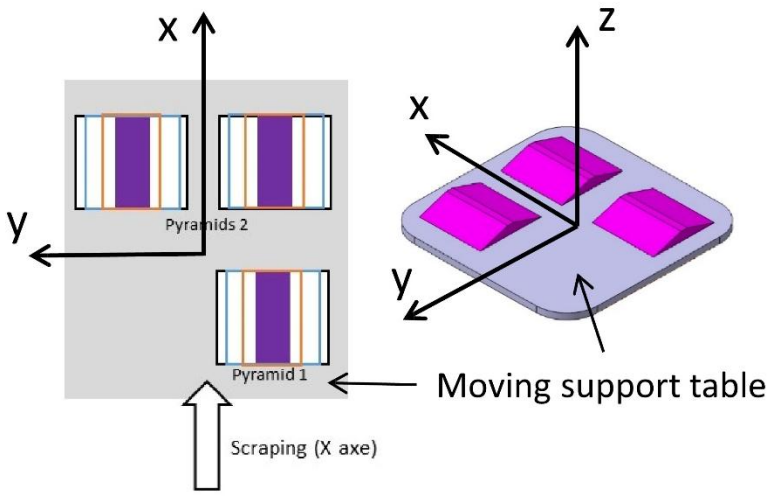


Fig. 5. Printed parts to quantify scraping loads

Loads in the scraping direction ($\vec{x}$ direction), represented in Fig. 6, are equal or lower than $1\,N$ whatever the layer considered. An increase of this load can be observed in the beginning of the support plate until the arrival of doctor blade for all layers. For the first pyramidal part, named 1, the load is constant for the layers from 0 to 5 (layer 0 = first layer) and decreases significantly for subsequent layers. Concerning the two last pyramidal parts, named 2, the load significantly increases for the layers from 0 to 5 number until the end of scraping step (the sign of the load changes during the scraping of pyramids 2). We can observe that the load applied on the layers 20 to 48 have the same evolution as those of pyramid 1. Finally, the loads are not dependent to the width of the part in the scraped layer. Moreover, in the first part of the scraping step, a mechanical action is generated in the scraping direction and when the scraper exceeds the middle of the plate, the mechanical action changes sign and opposes the scraping movement.

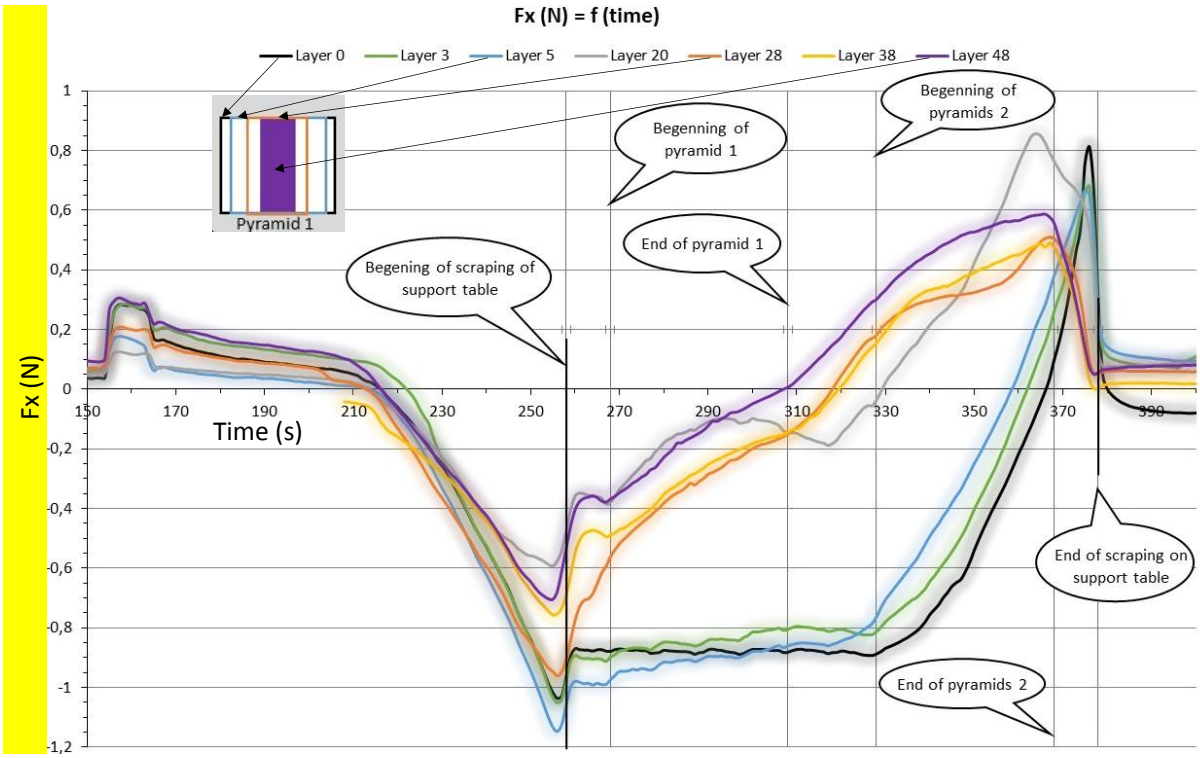


Fig. 6. Loads measured in the scraping direction ($\vec{x}$) according to time

Loads in normal direction to the support table ($\vec{z}$ direction), represented in Fig. 7, are higher than those in the scraping direction and present the same evolution independently from the scraped layer. The loads are constant and negative between the beginning of each printing of pyramidal parts 1 and 2. The presence of loads in the normal direction of the layer spreading direction means that the Couette flow model is not here valid. This hypothesis, used in literature for the tape casting process, is therefore not suitable to describe the rheological behavior of our curable ceramic suspension. It can be notified that there is not any load in the third direction ($\vec{y}$ direction) during the scraping process.

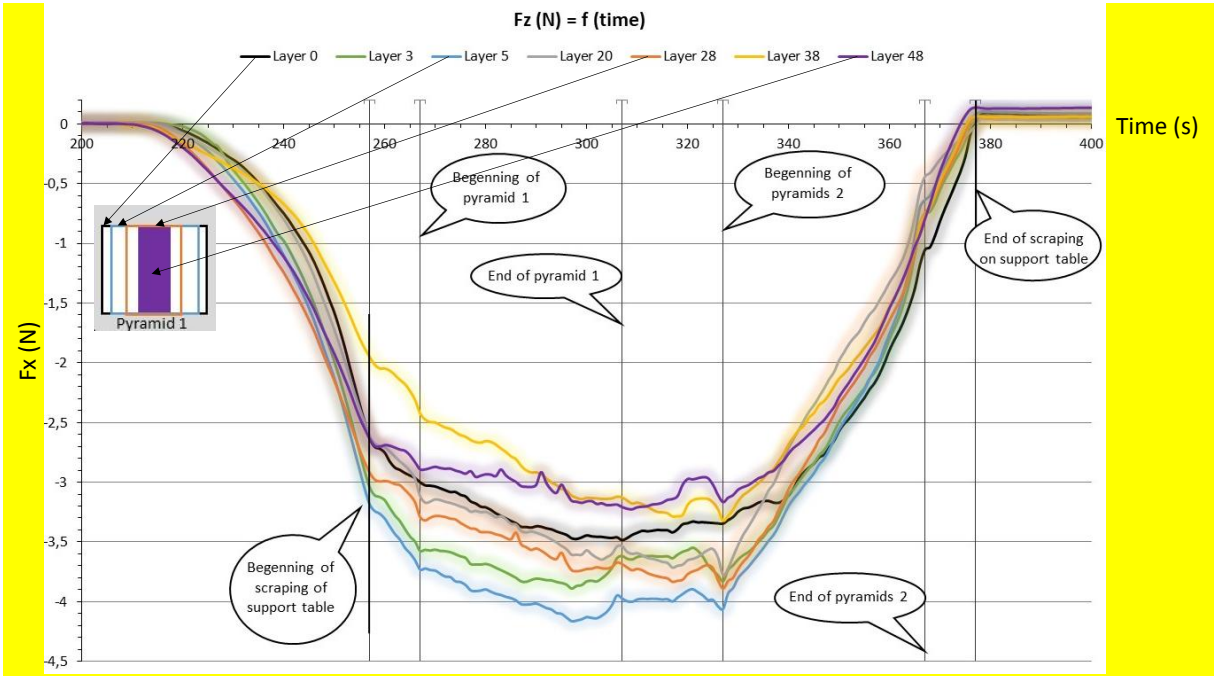


Fig. 7. Loads measured in the normal direction ($\vec{z}$) to scraping direction according to time

The analysis of loads imposed to the paste during the scraping step in the stereolithography process, then to the part in construction, has never been reported in literature. Even if this original study remains descriptive, it offers the advantage to evaluate the loads imposed by the blade doctor on a green part and its support via a ceramic paste during the stereolithography process. Results obtained by the design of experiments permit to choose a set of scraping parameters that minimizes the mechanical loads on the printed part in order to ensure a correct printing. For our suspension, the better parameters are, i) a scraping speed of 1 mm/s, ii) a high oscillations level of the doctor blade, iii) a layer thickness of 75 µm and, iiii) a paste quantity of 20 g.

Even if the mechanical loads due to the scraping process are minimized by choosing the best set of parameters, loads cannot be ignored. Then, the green parts are always subjected to compressive loads in the normal direction to the support table and to shear loads in the scraping direction. These loads can therefore have a direct impact on the mechanical resistance of the green parts and their supports and on a possible deformation, slippage or failure of the part during its construction.

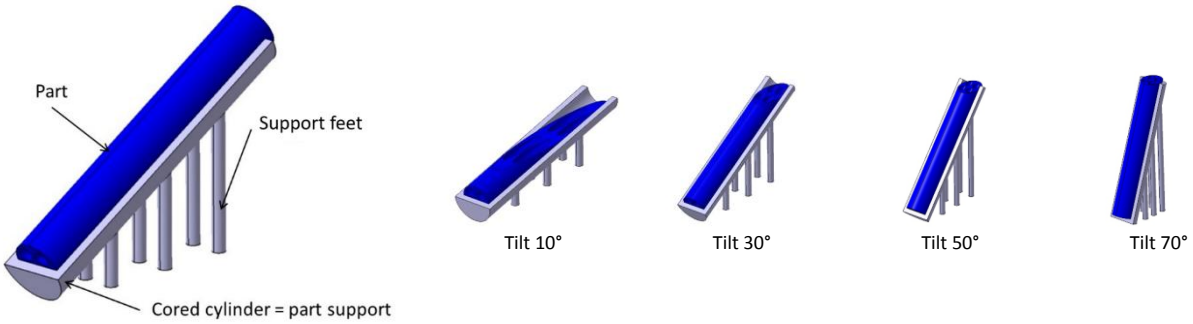
3. Finite elements modelling

3.1. Description and aims of modelling

In order to choose an optimal orientation of construction of the part on the stereolithography working plate to minimize its deformations, finite element simulations have been performed. These models permit to determine the relative displacements, in the loading directions ($\vec{x}$ and $\vec{z}$), of a part with

respect to its supports during the construction. Many orientations of the part, in particular tilts from 10° to 90°, have been evaluated in order to minimize the build time and the number of layers; these two parameters being dependent in the case of the stereolithography process. Moreover, the design of the supports has been also optimized in order to minimize the quantity of ceramic paste used during the printing.

The part tested is composed of a cylinder with a diameter of 15 mm and a height of 100 mm and 4 axial holes inside having a 5 mm diameter. The part is supported by a cored-cylinder structure with support feet. The part-support assembly and some orientations (tilts from 10° to 70°) of this assembly are represented in Fig. 8a and Fig. 8b, respectively. In order to study the influence of the orientation on the part building, it was chosen to keep an identical support in all cases, consisting of six evenly distributed feet on the entire floor surface of the support.



a) Green part and supports

b) Different orientations of the assembly

Fig. 8. Green part and supports assemblies

3.2. Mechanical behaviour, loading and boundary conditions

The mechanical behavior of the green part and its support, constituted of the same material, is considered linear elastic in order to simplify the modellings. The Young's modulus and the Poisson ratio are 1.8 GPa and 0.35, respectively. These mechanical properties correspond to a laser power, a laser velocity and a hatch spacing equal to 225 mW, 3500 mm/s and 20 μm, respectively [24].

The finite elements model imposed the following loadings and boundary conditions (Fig. 9):

- the load, described in the 2.2 section, is distributed over the surface of layer during building with $F_x = 1.5\ N$ and $F_z = 4\ N$;
- the support feet are embedded in the moving support table in order to simplify the modelling;
- a contact condition, with sliding and / adhesion, is considered between the part and its support;
- as part and support present a plane symmetry $(\vec{x}, \vec{z})$, a symmetric boundary condition is used to avoid rigid body motions.

As the part is not embedded in its support, sliding and adhesion conditions are chosen to model the contact. The values of friction coefficient, obtained from the normal and tangential forces measured

with the load sensor (Fig. 3), are between 0.15 and 0.35 and showed an important discrepancy. In the modellings, this coefficient will therefore be taken between 0.1 and 0.4.

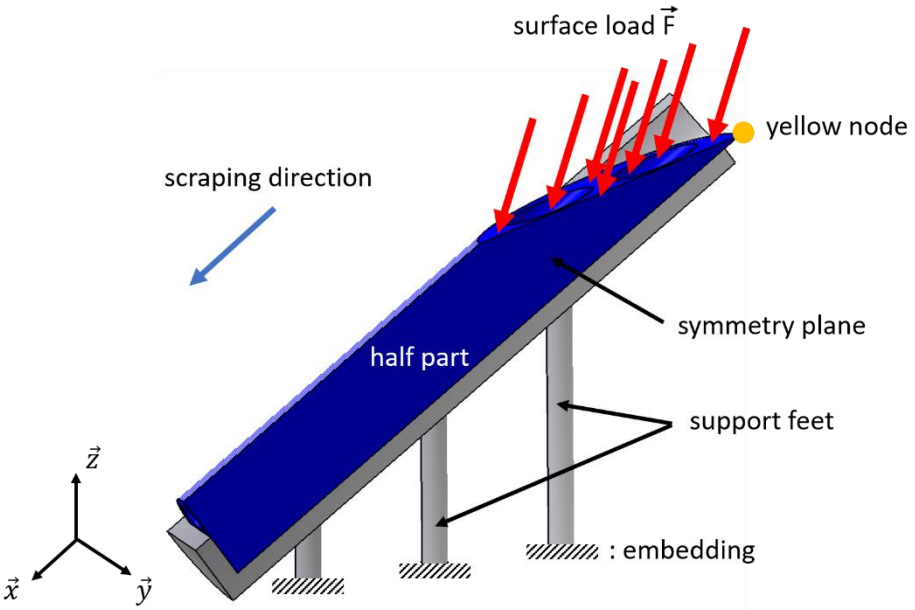


Fig. 9. Loading and boundary conditions of modelling

3.3. Results from modelling

The displacements were quantified in the $\vec{x}$ and $\vec{z}$ directions for a single node of the finite element model located at the top of the part in the layer under building (yellow node in Fig. 9). When the sign of load in the $\vec{x}$ direction is positive, the green part is compressed on to its support and leads to elastic deformation of the part-support assembly. In this case, it is important to minimize the part height to reduce stresses on the support and thus the displacements of the different elements; and the printing time too. On the other hand, when the sign of load in the $\vec{x}$ direction is negative, the green part may not adhere to the support and may move. The displacement values of the yellow node in the $\vec{x}$ direction, for different values of friction coefficient and for different tilt angles are given in Fig. 10. Whatever the friction coefficient value, for a tilt angle between 0 and 15° of the part-support assembly, the part slides into its support with very important values of displacement. From an angle of inclination of 20°, the greater the angle, the greater the height of the part-support assembly and the greater the displacement at the top of the part is. This result is completely consistent with the mechanical behavior of a structure stressed on its top. This tendency is identified regardless of the friction coefficient between the part and its support. In our case, the optimal tilting angle of the green part and its supports is equal to 20°. This angle value corresponds to the minimum height of the part on the moving support table that ensure a non-slippage of the part into its support and minimal printing time.

It is therefore necessary to sufficiently tilt the part-support assembly to prevent the green part from sliding in its support (Fig. 11 (a)) but it is also very important to minimize the tilt angle to limit part height and consequently the displacements due to stress generated by scraping loads (Fig. 11 (c)). The Von Mises stresses do not exceed 1.2 MPa whatever the tilt angle. The support feet are submitted to higher stresses than the green part. It will be therefore essential to pay particular attention to the stiffness of feet of the support to minimize the displacements of the green part.

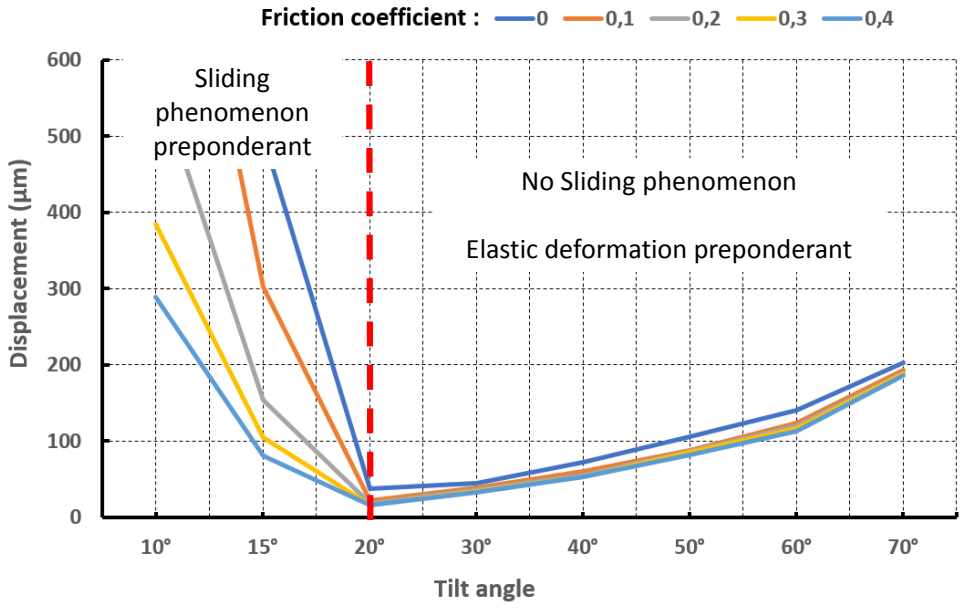
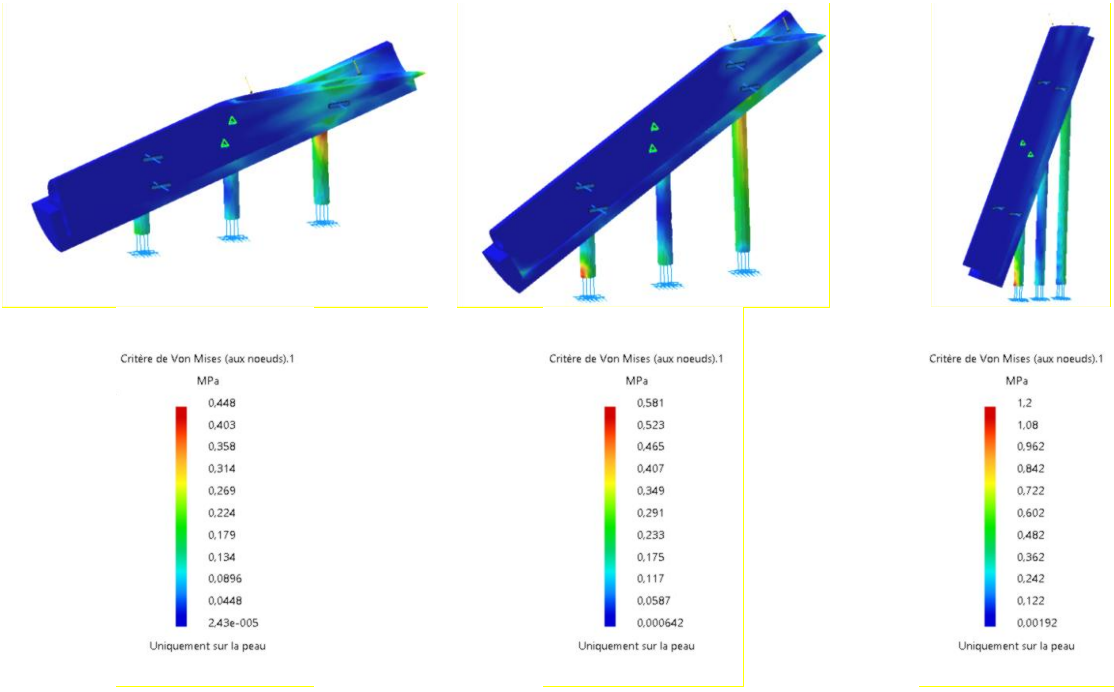


Fig. 10. Displacement in $\vec{x}$ direction according to support tilt for different values of friction coefficient



a) Tilt 15° b) Tilt 30° c) Tilt 70°

Fig. 11. Von Mises stresses distribution in the green part-support assembly for different tilt angles

The Von Mises stresses distribution and displacement field, for a tilt angle equal to 20° corresponding to optimal tilt angle, are presented in Fig. 12. The maximum Von Mises stress is lower than 0.7 MPa and is located in the foot of support, which is facing the load. The maximum displacement corresponding to the lifting of the part from its support in the positive $\vec{z}$ direction (Fig. 12 (b)), is observed to the bottom of the green part and its value corresponds to a layer thickness equal to 50 µm.

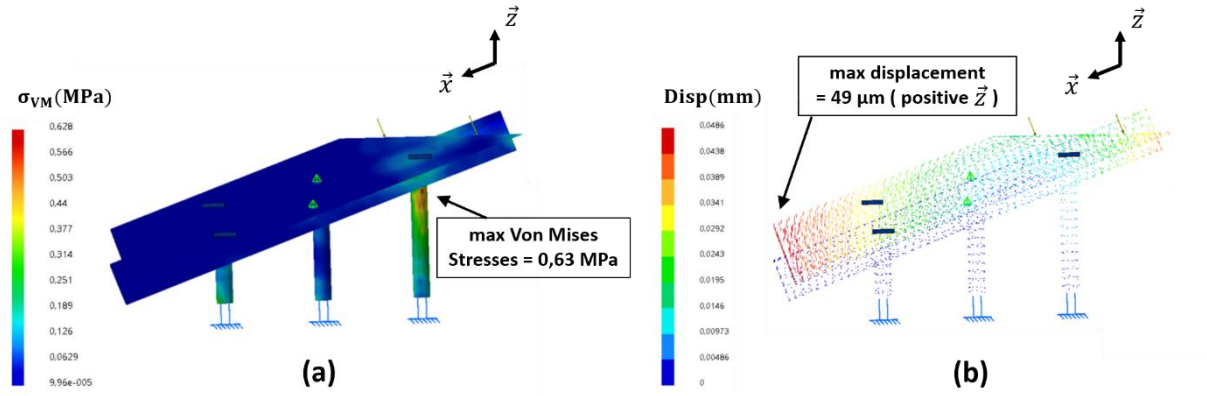


Fig. 12. Von Mises stresses distribution (a) and displacement field (b) in the green part-support assembly for a tilt angle equal to 20°

In order to quantify and to optimize the ceramic suspension quantity and minimize the green part displacement during scraping stage, several support designs have been modeled. The number and the diameter of support foot have been adapted. Fig. 13 (a) and Fig.13 (b) present two support design. The number of supports and their position are important parameters to minimize the displacement of the green part. Indeed, a support consisting of 5 feet of diameter equal to 4 mm leads to a lower displacement of the green part with respect to its support than 4 feet of diameter equal to 5 mm and results in a smaller amount of ceramic suspension. It is obvious that depending on the design of the support, the location of the maximum displacement will be different.

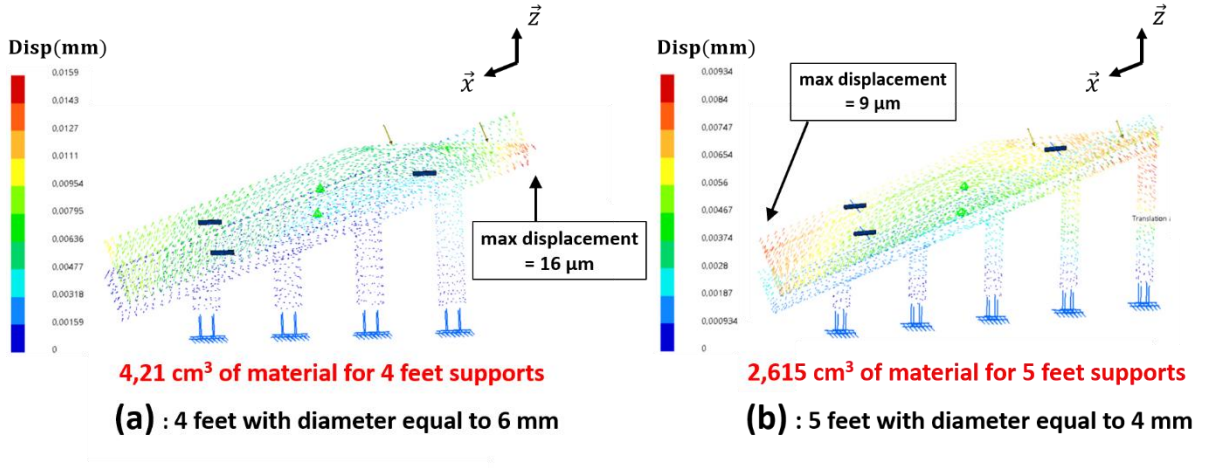


Fig. 13. Displacement field in the green part-support assembly for different designs of support feet

4. Discussion and conclusion

This study is focused on the identification of the loads that the green part undergoes during the spreading step of the ceramic suspension in the stereolithography process and on the optimal orientation of the part and its support in order to minimize the elastic deformations. The instrumentation of the stereolithography machine has shown, in particular, that preponderant loads are generated in the normal direction to printing direction. This observation, which is not intuitive has, to our knowledge, never been reported in the literature. This normal force can lead to the stressing of the part and its supports and therefore to a possible deformation or slippage of the part during its construction. Measurements of the loads during the spreading of the paste made it possible, in a first approach, to model by finite elements, the optimal orientation of the green part and its support. The exploitation of the results from modelling showed that it exists a specific orientation of the part that minimizes stresses then its deformation. In addition, the position of feet of the support can influence the deformation of the part as well as the amount of paste necessary to build the part-support assembly. The results from modelling also highlighted the importance of the rigidity of the supports that absorb the scraping forces. In order to improve the optimal orientation of the part-support assembly and the design of support, the mechanical behavior of the polymerized material (i.e. the visco-elastic behavior) constituting the green part and the support will have to be considered. In this respect, specific experimental measurements will have to be carried out in order to determine the viscoelastic properties of the green part. Moreover, particular attention should be paid to the nature of the contact surface between the green part and its support, which has a critical importance on the mechanical behaviour of part-support assembly. These improvements should lead to provide a direct link between the manufacturing parameters and the mechanical behavior of the green parts.

References

[1] P. J. Bartolo, Stereolitography: Materials, Processes and Applications, Chapter 6 – Materials of Stereolithography, Springer Science & Business Media, (2011), p. 141-160.

[2] T. Chartier, C. Chaput, F. Doreau, M. Loiseau, Stereolithography of structural complex ceramic parts, J. Mater. Sci., 37, (2002), 3141-3147.

[3] H. Wu, W. Liu, R. He, Z. Wu, Q. Jiang, X. Song, Y. Chen, L. Cheng, S. Wu, Fabrication of dense zirconia-toughened alumina ceramics through a stereolithography-based additive manufacturing, Ceram. Int. 43 (1) (2017) 968–972.

[4] J. Brie, T. Chartier, C. Chaput, C. Delage, B. Pradeau, F. Caire, M.P. Boncoeur and J.J. Moreau, A new custom made bioceramic implant for the repair of large and complex craniofacial bone defects, J. Cranio-Maxillo-Fac. Surg., 41, (2013), 403-407.

[5] J. Raynaud, V. Pateloup, M. Bernard, D. Gourdonnaud, D. Passerieux, D. Cros, V. Madrangeas and T. Chartier, Hybridization of additive manufacturing processes to build ceramic/metal parts: Example of LTCC, J. Eur. Ceram. Soc., 40, (2020), 759-767.

[6] S. Sakari, M. Vippola and E. Lavänen, A comprehensive review of the photopolymerization of ceramic resins used in stereolithography, Add. Manuf., 35, (2020), 101177, 1-14.

[7] T. Chartier, C. Dupas, P. M. Geffroy, V. Pateloup, M. Colas, J. Cornette and S. Guillemet-Fritschb, Influence of irradiation parameters on the polymerization of ceramic reactive suspensions for stereolithography, J. Eur. Ceram. Soc., 37, (2017), 4431-4436.

[8] T. Hafkamp, G. van Baars, B. de Jager and P. Etman, A trade-off analysis of recoating methods for vat photopolymerization of ceramics, Proceedings Solid Freeform Fabrication Symposium (2017), 687–711.

[9] A. Badev, Y. Abouliatim, T. Chartier, L. Lecamp, P. Lebaudy, C. Chaput and C. Delage, Photopolymerization kinetics of a polyether acrylate in the presence of ceramic fillers used in stereolithography – J. Photochemistry and Photobiology A: Chemistry, 222, (2011), 117-122.

[10] G. Gorso, S. Lo Casto, A. Lombardo and S. Freni, The influence of the tape-casting process parameters on the geometric characteristics of Sic tapes, Mat. Chem. and Phys, 56, (1998), 125-133.

[11] M. Svec, A. Roosen, M. Schmidt, H. Munstedt, Th. Betz and F. Koppe, The influence of different blade geometries on the local flow behavior of ceramic slurries in the tape casting unit, Ceramic Forum International, 79, (5), (2002), 6 p.

[12] P. Polfer, Z. Fu , T. Breinlinger A. Roosen and T. Kraf, Influence of the Doctor Blade Shape on Tape Casting - Comparison Between Analytical, Numerical, and Experimental Results, J. Am. Ceram. Soc., 99, (10), (2016), 3233-3240.

[13] B. Timurkutluk, S. Celik and E. Ucar, Influence of doctor blade gap on the properties of tape cast NiO/YSZ anode supports for solid oxide fuel cells, Ceram. Int., 45, (3), (2019), 3192-3198.

[14] W. Cheng, J.Y.H. Fuh, A.Y.C. Nee, Y.S. Wong, H.T. Loh and T. Miyazawa, Multi-objective optimization of part-building orientation in stereolithography, Rapid Prototyp., 1, (4), (1995), 12–23.

[15] P.T. Lan, S.Y. Chou, L.L. Chen and D. Gemmill, Determining fabrication orientations for rapid prototyping with stereolithography apparatus, Comput. Aided Des., 29, (1), (1997), 53–62.

[16] P. Alexander, S. Allen and D. Dutta, (1998), Part orientation and build cost determination in layered manufacturing, Comput. Aided Des., 30, (5), (1998), 343–356

[17] F. Xu, H.T Loh and Y.S Wong, Considerations and selection of optimal orientation for different rapid prototyping systems, Rapid Prototyp., 5, (2), (1999), 54–60.

[18] P. Das, R. Chandran, R. Samant and S. Anand, Optimum part build orientation in additive manufacturing for minimizing part errors and support structures, Procedia Manuf., 1, (2015), 343–354.

[19] P. Delfs, M. Tows and H.J. Schmid, Optimized build orientation of additive manufactured parts for improved surface quality and build time, Addit. Manuf. ,12, (2016), 314–320.

[20] F. Liravi, S. Das and C. Zhou, Separation force analysis and prediction based on cohesive element model for constrained-surface Stereolithography processes, Comput. Aided Des., 69, (2015), 134‐142.

[21] X. Wu, Q. Lian, D. Li and Z. Jin, (2017), Tilting separation analysis of bottom-up mask projection stereolithography based on cohesive zone model, J. Mater. Process. Technol., 243, (2017), 184‐196.

[22] T. Hada, M. Kanazawa, M. Iwaki, T. Arakida, Y. Soeda, A. Katheng, R. Otake and S. Minakuchi, Effect of Printing Direction on the Accuracy of 3D-Printed Dentures Using Stereolithography Technology, Mat., 13, (3405), (2020), 12 p.

[23] 3D Ceram (Limoges, France- http://3dceram.com)

[24] P. Michaud, V. Pateloup, J. Tarabeux, A. Alzina, D. André and T. Chartier, Numerical prediction of elastic properties for alumina green parts printed by stereolithography process, J. Eur. Ceram. Soc., 41, (2021), 2002-2015.